Inverse Dynamics of a Swimmer Multibody Model: An Analysis of the Lower Limbs During Front Crawl

Mariana Sequeira
marianafsequeira@tecnico.ulisboa.pt
Instituto Superior Técnico, Universidade de Lisboa, Portugal
January 2021

ABSTRACT

The present work aims to propose a full body model representation of the human body to conduct an inverse dynamic analysis of the lower limbs during swimming activities. Considering multibody dynamics, a three-dimensional biomechanical model using Cartesian coordinates is presented.

Kinematic data provided by Porto Biomechanics Laboratory (LABIOMEP-UP) are collected for a male swimmer performing the six-beat front crawl swimming. The external forces describing the interactions between the human body and surrounding environment were estimated using a computer simulation method available in the literature. An interface between the full body biomechanical model and the simulation software is developed to perform (1) the conversion of body geometry specifications and motion data, that is given as input to the simulation, and (2) the processing of the simulation output data containing the external forces, that are addressed to the full body model. Inverse dynamic analyses are performed considering the full body biomechanical model actuated upon by driver actuators, referred to as determinate problem, to evaluate the joint torques and intersegmental joint forces acting on the human lower limbs.

The kinematic results, which are generally in good agreement with the literature, provide confidence about the consistency between both laboratorial and model data. The motion of the human lower limbs during front crawl swimming is described as an alternate rhythmical movement upwards and downwards, respectively denoted as upbeat and downbeat. However, as far as the interface developed is concerned, the results show some discrepancies on the force magnitudes acting upon the feet during some phases of the stroke cycle. It is expected that these discrepancies have impact on the intersegmental joint forces and joint torques of the lower limbs, although the lack of literature in this field of research does not allow a complete validation of results. Nevertheless, the results of the determinate problem are presented and discussed for the anatomical joints of the human lower limbs.

Keywords: Biomechanics, Front crawl stroke, Hydrodynamic forces, Inverse dynamics, Joint torques, Lower limbs, Multibody dynamics, Swimming analysis.

1 INTRODUCTION

Biomechanics is the field of science that describes, analyses, and assesses the physiology of living structures and animals using the laws of mechanics. Human motion is one of the objects of study in biomechanics (Winter, 2009), which involves complex interactions between the neuromuscular and skeletal systems. Understanding these interactions is necessary for the diagnosis and treatment of patients with motor deficiencies and to enhance performance of able-bodied individuals (Rajagopal et al., 2016). Fundamental quantities of interest in human motion research are the intersegmental forces and moments acting at the joints, which represent the net loads that act at each biomechanical joint (Derrick et al., 2020). Computational biomechanical models based on multibody dynamics are powerful tools that enable the evaluation of these quantities in the human body, whose *in vivo* or *in vitro* measurement is, when possible, extremely difficult (Quental et al., 2015). In the context of human swimming, current biomechanical models are mostly based on simplified models of specific parts of the human body (Cohen et al., 2015; Lauer et al., 2016). Due to limitations on motion acquisition, especially in the

air-water interface, they are kept simple and are hardly able to simulate the broad range of motion of many of the anatomical segments relevant to swimming.

Another fundamental data for the evaluation of internal forces are the external forces acting on the human body during swimming, herein referred to as hydrodynamic forces. Unlike terrestrial motion where these external forces are easily measured using force platforms, the determination of the external forces in water is very difficult (Lauer et al., 2016). Although advances have been made in the development of pressure measurement equipment, their application is still very limited to specific body segments, and do not precisely reflect the instantaneous points of force application (Takagi and Sanders, 2002). Over the last decades, the use of computational fluid dynamics (CFD) and smoothed-particle hydrodynamics methods (SPH) has emerged in aquatic locomotion research as a promising alternative of determining all the important quantities and thus provide insight into swimming hydrodynamics. Both methods are based on fundamental fluid mechanics principles. However, they are computationally and time expensive, given the complexity of simulating the dynamically changing shape, with rotations of many body segments about multiple axes, and the large deformation of the water surface (Takagi et al., 2015). Nakashima et al. (2007) developed an alternative computer simulation tool that requires much less computation time. The simulation software Swumsuit determines the fluid forces acting on each segment of the whole body, without solving the flow field. Instead, they are determined from the local kinematics of each part of the human body at each instant of time, and from the force coefficients estimated experimentally (Nakashima et al., 2007).

In this work, a multibody biomechanical model representing the full human body, the Lisbon Human Body Model (LHBM), is applied in an inverse dynamic analysis to evaluate the intersegmental joint forces and joint torques of the human lower limbs during a six-beat front crawl swimming stroke. To perform an inverse dynamic analysis, the motion of the multibody system must be known in advance as well as the externally applied forces so that the only unknowns are the internal forces (Nikravesh, 1988). The kinematic data of the swimming motion performed by a male subject are provided by LABIOMEP-UP. The external hydrodynamic forces are determined with the simulation software Swumsuit. The second aim is to develop an interface between the simulation software and the LHBM that performs the adjustment on the software inputs and outputs to properly fit the characteristics between the LHBM and the simulation Swimming Human Model (SWUM). The interface is developed on a general basis to allow future studies to be conducted for front crawl or any other swimming technique supported by Swumsuit.

2 METHODS

2.1 Biomechanical Model

The 3D full body model of the human body is composed of sixteen rigid bodies, including the pelvis, torso, neck, head, and right and left thighs, legs, feet, arms, forearms, and hands. The body segments are constrained by fifteen anatomical joints: eight spherical joints represent the cervical, lumbar, and right and left hip, shoulder, and ankle joints; four universal joints represent the right and left elbow and wrist joints, and three revolute joints represent the right and left knee, and the atlanto-occipital joints (Oliveira, 2016). The multibody system has a total of 41 (DOF): six describe the position and orientation of the pelvis with respect to the global reference frame, which is responsible for the motion of the human body model as one whole, while the remaining 35 DOF are related to the relative motion of body segments at the kinematic joints.

The computation of the body segment inertial parameters of the biomechanical model follows the dataset of scaling equations proposed by Dumas et al. (2007a, 2007b), except for the head and neck body segments, which are defined according to Pàmies-Vilà (2012). The kinematic data provided by LABIOMEP-UP are obtained for a 25-year-old male swimmer with 70.3 kg, and 1.80 m. By following the dataset of Dumas et al. (2007a, 2007b) no further scaling procedures are required to match the characteristics of the anthropometric model and those of the swimmer subject.

2.2 Kinematic Consistency

Data acquisition for a six-beat front crawl swimming stroke was conducted in LABIOMEP-UP using a three-dimensional motion capture system. Given the nature of motion, the capture system comprised a set of underwater and above-water cameras. The kinematic data provided consist in the trajectory of reflective markers placed on anatomical landmarks of the swimmer's surface body in the global frame. The orthogonal axes of the global frame define X in the lateral direction, Y in the direction of swim, and Z in the vertical direction. A total of 38 markers are used to define the biomechanical model described in Section 2.1. Considering a Cartesian coordinates formulation, the body-fixed, or local, reference frame of each body segment is defined following the recommendations of the *International Society of Biomechanics* (ISB) (Wu et al., 2002, 2005). After proper filtering of the kinematic data to remove noise, a kinematic analysis is performed to ensure the calculation of consistent positions, velocities, and accelerations between both laboratorial and model data (Silva and Ambrósio, 2002). The kinematic constraints of the multibody system must be satisfied, such that:

$$\boldsymbol{\Phi}(\mathbf{q}, t) = \mathbf{0} \tag{1}$$

where $\boldsymbol{\Phi}$ represents the vector of constraint equations of the multibody system, $\mathbf{q}$ is the global consistent positions vector, t is the instant of time, and $\mathbf{0}$ is the null vector.

2.3 Estimation of the Hydrodynamic Forces

In this work, the simulation software Swumsuit, developed by Nakashima et al. (2007), is used to obtain the hydrodynamic forces acting upon the swimmer's body during a six-beat front crawl swimming. The human body model, denoted as SWUM, is represented as a series of twenty-one truncated elliptic cones. The unsteady fluid force components acting on each truncated elliptic cone include the inertial force due to added mass of fluid (Fa), normal (Fn) and tangential (Ft) drag forces, and buoyancy (Fb), which includes the gravitational forces. The fluid forces are obtained without solving the flow field. Instead, inertial force, and normal and tangential drag components are determined from the local kinematics of each part of the human body at each instant of time, and from the force coefficients, Ca, Cn, and Ct, respectively, which are estimated experimentally by Nakashima et al. (2007). Each truncated elliptic cone is divided into thin elliptic plates along the longitudinal axis, and all fluid force components except buoyancy are assumed to act on each centre of the thin elliptic plates. Buoyancy, on the other hand, is calculated by integrating the pressure force due to gravity acting on tiny quadrangles into which the side surface of the thin elliptic plate is divided in the circumferential direction.

2.3.1 Interface between Swumsuit and LHBM

As simulation input, the analysis engine part reads nine files, each containing data of body geometry, joint motion, analysis settings, and the absolute body motion, which is given by the three linear and three angular velocities of the whole-body COM at all instants of time of the stroke cycle. The first obstacle in the application of Swumsuit is the different discretisation of the human body model, as 21 versus 16 body segments are used to represent SWUM and LHBM, respectively. Therefore, a relationship between body segments is defined. Accordingly, the results of the kinematic consistency achieved in Section 2.2 of this work are converted to the simulation modelling specifications.

Once the simulation is finished, data output from Swumsuit must be processed to be consistent with the biomechanical model developed in this work and its formulation. Two types of force files are generated: 63 files (21 body segments × 3 force components) containing the total forces acting at the COM of each body segment, and a force file, denoted as `motion.dat` in Swumsuit, containing the forces acting at the centre of each thin plate, except buoyancy. The force data in the 63 files provide the global forces that are converted from SWUM to LHBM by performing the same relationship between body segments mentioned in the previous paragraph, and by applying a rotation matrix to transform from SWUM to LHBM global frames. The local moments are determined from the force data in `motion.dat`. However, in this file, the component of buoyancy is not considered. Thus, the force data in the 63 files are used to find the component of buoyancy missing. In addition, the force data in `motion.dat` is described in a different, non-stationary, coordinate system of that of

the 63 files. Therefore, the distributed forces acting along the longitudinal axis of each truncated cone are firstly transformed from the non-stationary coordinate system to the reference frame of the 63 force files. Then the component of buoyancy missing is determined and added to the distributed forces. Finally, these forces are transformed from SWUM to LHBM global reference frames. Each force applied in its application point of the longitudinal axis produces a moment in relation to the body segment COM. Finally, the total local moment of each body is the sum of the contribution of the 10 thin plates, expressed in the body-fixed reference frame of LHBM. Figure 1 addresses the procedure implemented computationally to convert modelling specifications and motion data from LHBM to SWUM, and vice versa.

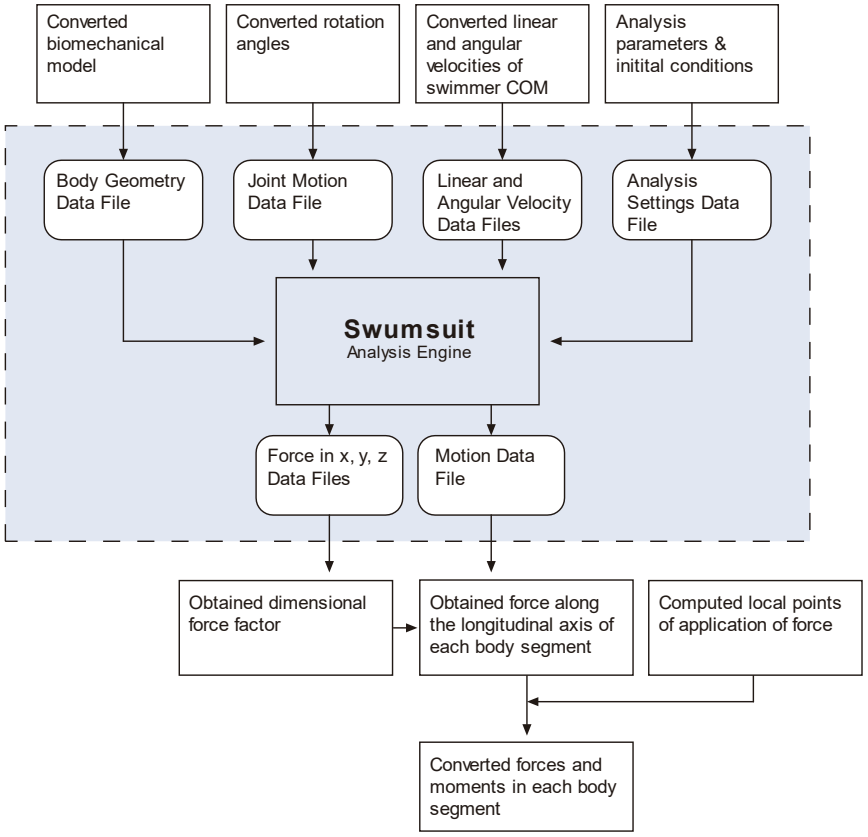

Figure 1: Data flow of the interface between Swumsuit and LHBM to perform kinetic data processing. The blue shaded rectangle represents the simulation analysis that is performed in Swumsuit.

2.4 Inverse Dynamic Analysis

Each kinematic joint introduces internal contact forces between the connected body segments. These can be expressed in terms of the constraint equations of the multibody system since they represent the forces produced by the biomechanical model that ensure the mechanically consistency with a pre-defined dynamic response. An inverse dynamic analysis is performed in MATLAB (Mathworks, Natick, MA) considering a fully determined problem, in which the DOF of the biomechanical model are actuated by drivers actuators. The equations of motion are given by:

$$\mathbf{M}\ddot{\mathbf{q}} + \boldsymbol{\Phi}_{\mathbf{q}}^{\mathrm{T}}\boldsymbol{\lambda} = \mathbf{g} \tag{2}$$

where $\mathbf{M}$ is the global mass matrix of the system, $\ddot{\mathbf{q}}$ is the vector of global consistent accelerations, $\boldsymbol{\Phi}_{\mathbf{q}}^{\mathrm{T}}$ is the Jacobian matrix, $\boldsymbol{\lambda}$ is the vector of Lagrange multipliers associated with the intersegmental forces developed by the kinematic constraints, and $\mathbf{g}$ is the vector of externally applied forces, containing, for each body, three entries regarding the global forces, and the three local moments mentioned in Section 2.3.1. In an inverse dynamics approach, Equation (2) is solved for the vector of Lagrange multipliers, which are the only unknowns of the system of equations.

3 RESULTS

The left-hand stroke is studied in this work since no loss of reflective markers registration during that period has been observed. The angles between body segments associated with the DOF of the biomechanical system are measured by processing the reflective markers acquired kinematics. Subsequently, these angles are prescribed in the LHBM using rotational drivers. The driving angles of the human lower limbs were compared with the literature (Nakashima et al., 2007), to validate the kinematic consistency of the swimming motion. However, since this work aims to evaluate the dynamic response of the motion of the lower limbs, these results are not presented here.

3.1 Simulation Software Swumsuit

The results of the simulation performed in Swumsuit of the six-beat front crawl swimming motion are presented in Figure 2 for six events of the stroke cycle. These events are identified by the corresponding percentage of the total stroke cycle time. The red arrows represent the direction and magnitude of the fluid forces acting on the swimmer's body segments, except buoyancy.

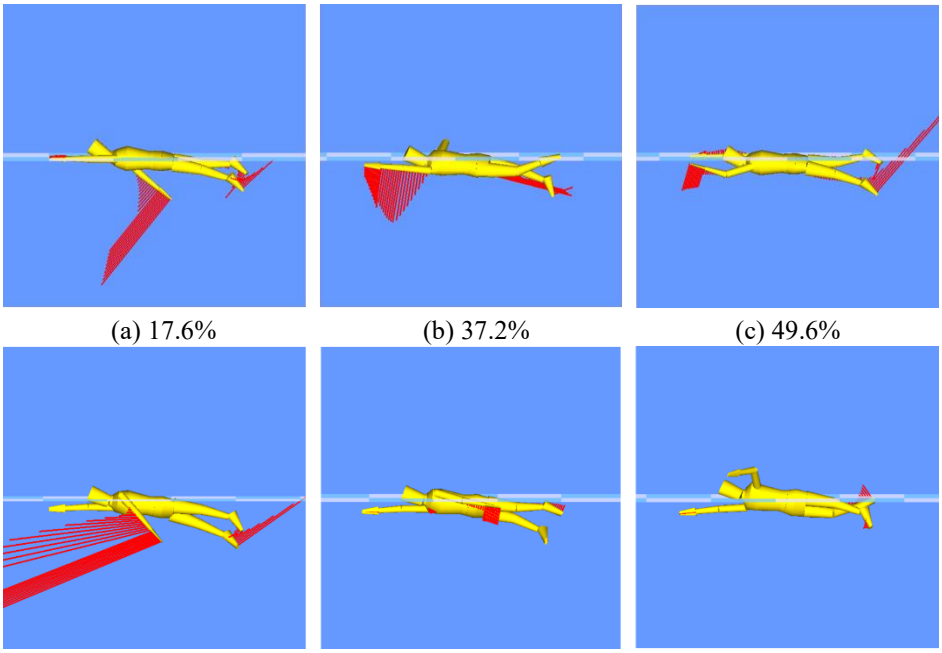

(a) 17.6% (b) 37.2% (c) 49.6%

(d) 63.2% (e) 71.2% (f) 90.4%

Figure 2: Simulation results of the left-hand six-beat front crawl swimming motion in Swumsuit. The six events are identified by the corresponding percentage of the total stroke cycle.

The global X, Y, and Z fluid force components acting upon the right foot, leg, and thigh body segments of LHBM are shown in Figure 3. These results are compared to those obtained by Nakashima et al. (2007). Although the force profiles are similar among the bodies of the right lower limb, their magnitudes are generally higher in the current study than those reported in the simulation performed by Nakashima et al. (2007), especially in the three components of the foot body segment.

Regarding the fluid forces acting on the right foot, three force peaks can be clearly identified in the vertical component, each acting approximately at 28%, 60%, and 99% of the stroke cycle, which is consistent with the motion towards the bottom of the swimming pool a few instants before, approximately at 20%, 51%, and 90%, which corresponds to frames (a), (c), and (f) in Figure 2. These instants of time are coincident in Figure 3 with the beginning of generation of propulsive force by the respective body, and the peak force is then reached a few instants later. The correlation of these peaks with the right ankle joint motion verifies the postulated assumptions in the literature that state that the maximum propulsive forces in the lower limbs occur during the downbeat, when the ankle in maximum plantarflexion (Keys, 2010; Sanders et al., 2017; Wei et al., 2014). On the other hand, the axial and lateral force components developed at the right foot are significantly

more relevant than those developed at the thigh and leg body segments. However, in the vertical component, the peak force of the right thigh and right leg in the LHBM are, respectively, 80.3 N and 44.3 N, against 71.2 N and 37.7 N reported by Nakashima et al. (2007). Although the maximum vertical force of 103.3 N remains in the right foot, the contribution of the remaining bodies is also important for thrust force generation of the lower limbs, which reinforces the importance of entire leg movement and positioning rather than just focusing on feet propulsion (Keys, 2010).

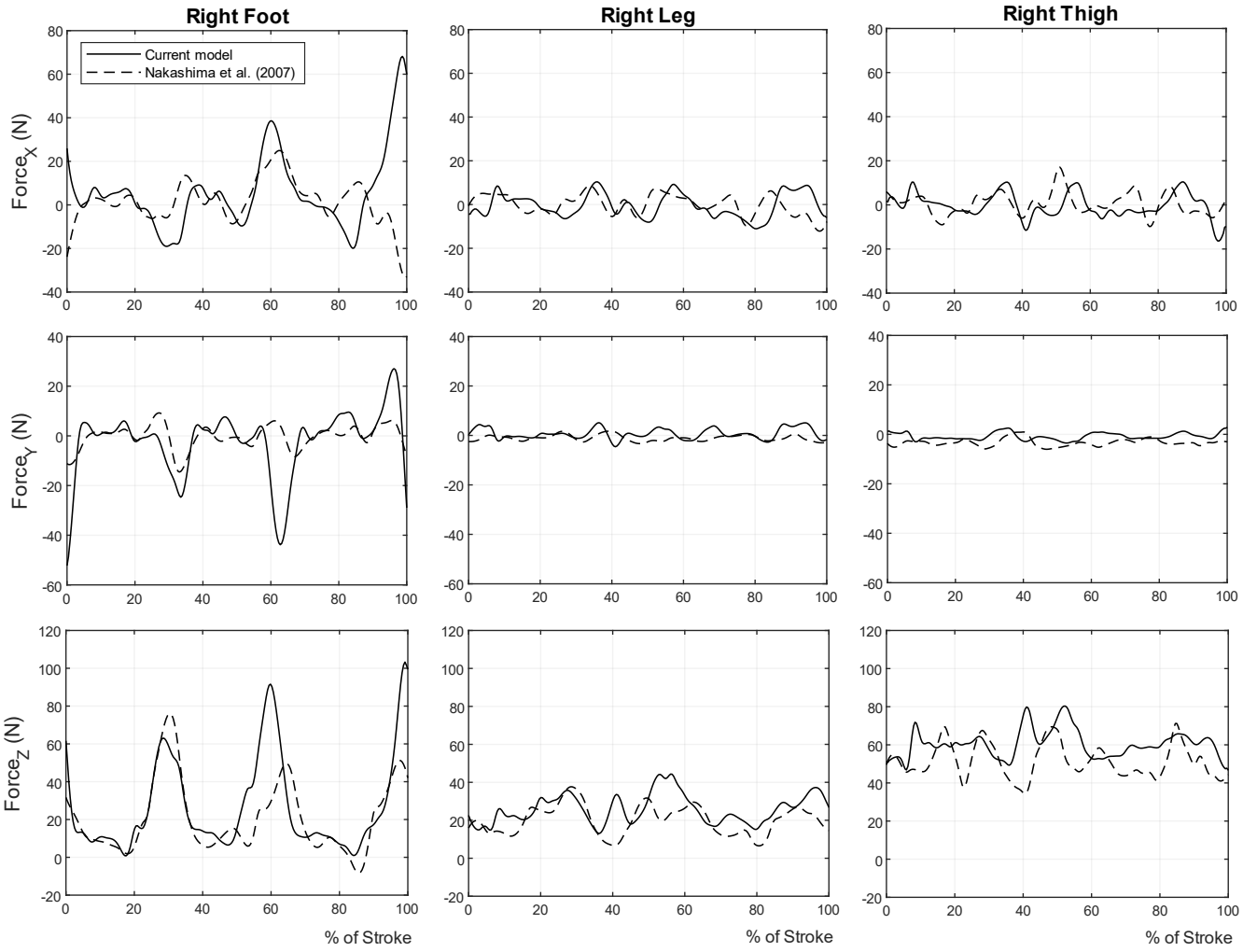

Figure 3: Simulation results of the hydrodynamic forces developed during a left-hand six-beat front crawl swimming stroke cycle. The horizontal axis corresponds to a percentage of the stroke cycle.

3.2 Solution of the Determinate Inverse Dynamic Analysis

The internal product of the vector of Lagrange multipliers by the transpose of the Jacobian matrix of the multibody system in Equation (2) provides the intersegmental joint forces and joint torques developed by the driver actuators at the kinematic joints. Figures 4 and 5 show the profile and magnitude of these quantities for the hip, knee, and ankle joints, during the six-beat front crawl swimming motion studied in this work.

The results obtained in the current work in Figure 4 show that the intersegmental forces of the right and left joints of the lower limbs are never null. However, for the knee and ankle joints, their value is very small during some intervals of the stroke (3-18%, 44-49%, and 68-84% for the right lower limb; 20-38%, 52-68%, and 95-100% for the left lower limb). Furthermore, the magnitude of the intersegmental forces at the right knee and ankle joints ranges from nearly 0 to 150 N and 125 N, respectively, as seen in Figures 4(b) and (c), while the right hip joint forces are up to 225 N. On the other hand, the results of the external hydrodynamic forces shown in Figure 3 verified that the higher forces occur at the foot. This

shows that peak loads at the kinematic joints are not uniquely due to the magnitude of the external hydrodynamic forces acting upon the adjacent body segments. If it was so, the results of the ankle joint forces should correspond to the highest magnitudes. In fact, the intersegmental forces are dependent on the combined effects of the external hydrodynamic forces plus the active joint forces necessary for controlling the joint motion, in this case, hip, knee, and ankle flexion and extension (Scott and Winter, 1990). The leg kick is described as a wave-like motion that begins with the extension/flexion of the thigh at the hip, and follows through the leg and foot, i.e., in the direction of proximal to distal joints (Keys, 2010). Being the hip the first element of the kinematic chain of the human lower limbs, higher intersegmental forces are concentrated at this joint. Despite the intra-cycle variations among joints, the comparison between the intersegmental force amplitudes of the - right and the left sides is very similar for all joints.

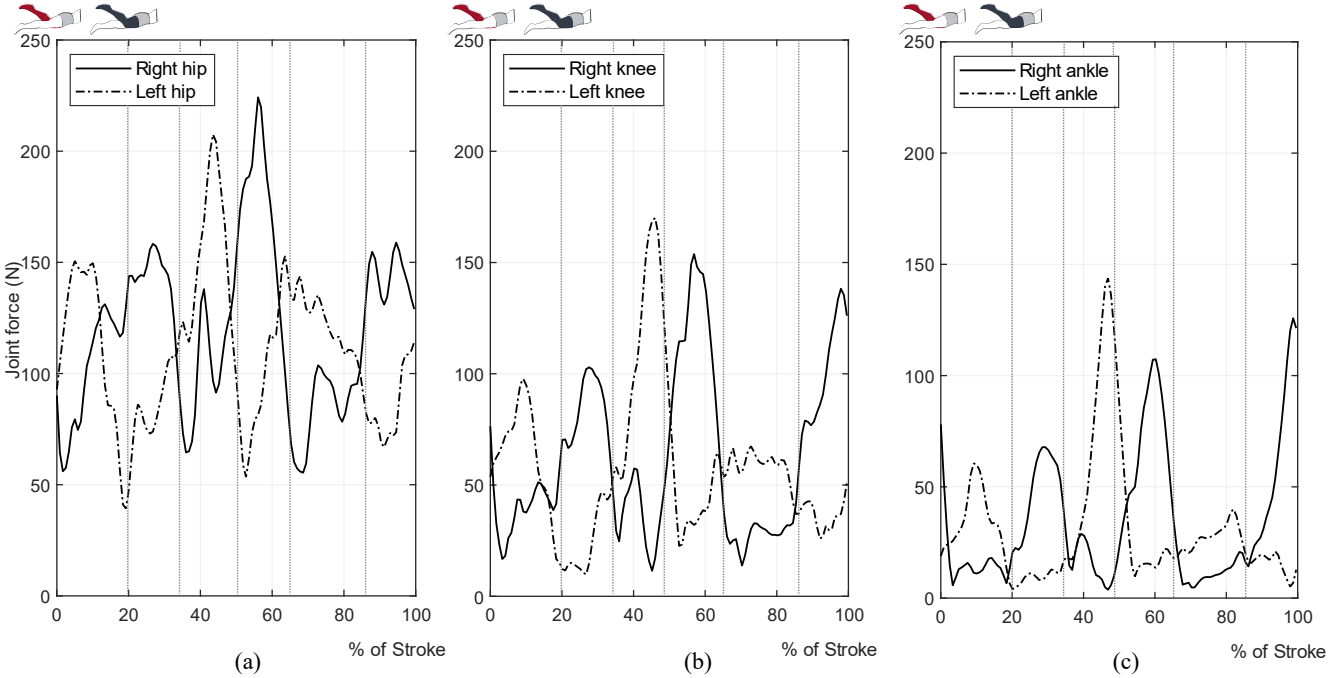

Figure 4: Intersegmental joint forces magnitude obtained during a left-hand six-beat front crawl swimming stroke cycle in the a) hip, b) knee, and c) ankle joints. The horizontal axis corresponds to a percentage of the stroke cycle.

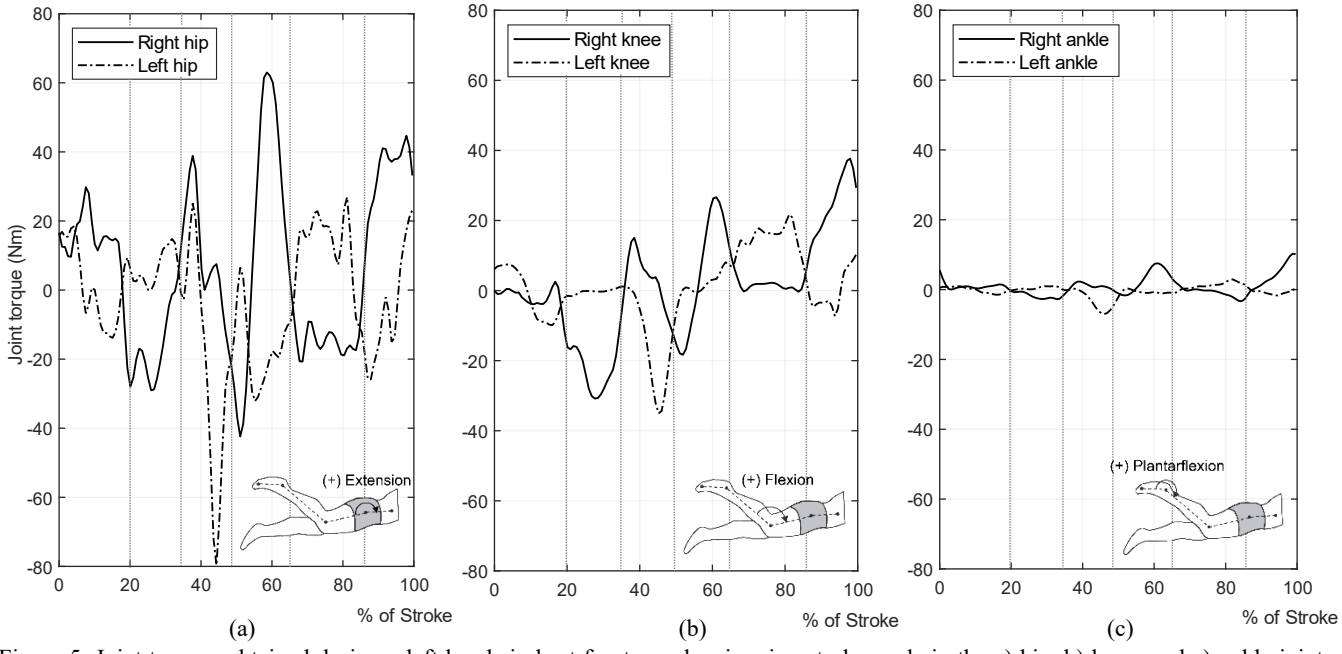

Figure 5: Joint torques obtained during a left-hand six-beat front crawl swimming stroke cycle in the a) hip, b) knee, and c) ankle joints. The horizontal axis corresponds to a percentage of the stroke cycle.

The convention for the joint toques is depicted at the right bottom of the respective joint in Figure 5. The stroke cycle under analysis begins with the downbeat of the left lower limb. In Figure 5(a), the left hip joint torque changes from positive to negative, while the hip is flexing and moving towards the bottom of the swimming pool. Accordingly, the left leg follows the thigh, and the left knee is extended (negative joint toque in Figure 5(b)). The left ankle joint torque in Figure 5(c) is approximately zero during the first half of the downbeat (0-10%) and becomes negative during the second half (10-20%), which means that the articular moment has the opposite direction (dorsiflexion). Simultaneously, the right lower limb performs the upbeat. Therefore, the right hip joint torque is positive as the right thigh moves upwards (hip extension), and the right knee changes from negative to positive torques while flexing. During the same interval, the right ankle joint torque becomes positive. Since the motion of the lower limbs is cyclic, the same pattern is repeated throughout the stroke cycle, alternating between upward and downward movement of each leg.

4 DISCUSSION

The results obtained in this work allow the identification of six phases during the stroke cycle, which are characteristic of a six-beat front crawl technique. Each lower limb performs three upbeats and three downbeats, and the upward sequence of one leg is coordinated with the descending sequence of the counter leg.

Despite the similarity regarding the distribution of fluid forces throughout the stroke cycle shown in Figure 3, the force magnitudes obtained in the current work are larger, by more than 40 N, than those reported by Nakashima et al. (2007). Three possibilities are identified as possible sources of error. The first hypothesis is that higher flexibility of the ankle joint induces high propulsion developed by the foot (Keys, 2010). The second hypothesis is related with the combined action of body roll, i.e., the rotation of the swimmer's body along the longitudinal axis, and leg kick motion. In Figure 2, the transition of the swimmer's body rotation from the right to the left side occurs between instants depicted in frames (c) and (d). At that same time, the downbeat of the right leg is initiated, as it moves from the top position in (c) to the bottom in (d). Simultaneously, the vertical force in the right foot increases, as shown in Figure 3. The combined rotation of the swimmer's body to the left side and the kicking action of the right leg in the same direction could result in a higher peak of force obtained in the Z component of the right foot. Lastly, in swimming motion analysis, the unsteady fluid forces are often more important due to the relatively high accelerations of the body segments. Swimmers are constantly changing the velocity and position of body segments to enhance swimming efficiency. As the pelvis linear and angular accelerations are given as input to the simulation analysis, it is possible that the acceleration of body segments is higher in this work than that obtained by Nakashima et al. (2007), and consequently the forces developed are higher.

Regarding the results of the inverse dynamic analysis, the larger and smaller peaks in Figure 4, correspond, respectively, to the three downbeats and three upbeats of each leg. During the upbeat, occurs extension of the thigh at the hip, followed by the upward motion of the leg and foot (Keys, 2010). Consequently, these bodies reach a position near the water surface and the joint force decreases. The same occurs during the entry of the hand into the water, as reported by Harrison et al. (2014), that analysed the joint torques for the arms of a male swimmer performing the front crawl stroke. If the ankle and knee joint forces are compared at the instants depicted in Figure 2, it can be observed that their magnitudes are lower when the body segments move closer to the water surface. Furthermore, the development of larger peaks during the downbeat of the lower limbs is consistent with the analysis of the external forces developed for the right lower limb, since during this phase the force created by the surrounding water over the body parts of the lower limbs is higher, propelling the body forward.

In general, the results for the hip and knee joint torques show agreement throughout the cycle for both sides of the lower limbs since its variation is consecutively alternating according to the downbeat and upbeat sequences. However, the variation of the right and left ankle joint torques does not follow the expected behaviour throughout the entire stroke cycle. During the first half (0-50%), the joint torques are negative on the downbeat (dorsiflexion), and positive during the upbeat (plantarflexion) of the respective lower limb, but during the second half cycle (50-100%) they change to the expected variation. For instance, the second downbeat of the right leg begins at approximately 51% of the cycle and lasts until 64%. During this interval, the right lower limb moves downwards. The external hydrodynamic forces acting upon the right foot have the opposite direction of motion, which contributes to a positive moment at the right ankle joint, and therefore

corresponding to a positive torque in Figure 5(c). A possible reason for the incongruity during the first half cycle is due to the external hydrodynamic forces acting upon the foot, i.e., although the foot is in plantarflexion during the down kick, the external forces cause a negative joint torque at the ankle joint. Nevertheless, the ankle joint torques are one order of magnitude lower than those for the hip and knee joints, and analogously to the intersegmental forces, the joint torques are of greater magnitude for the hips.

5 CONCLUSIONS AND FUTURE WORK

A full-body model of the human body was proposed for inverse dynamic analysis of the lower limbs. To overcome the limitations on the acquisition of the external forces acting on the human body, the simulation software developed by Nakashima et al. (2007) was used to determine the hydrodynamic forces, allowing the computation of the intersegmental joint forces and joint torques. The results of the external hydrodynamic forces support the validity of the interface developed between Swumsuit and the LHBM, as the dynamic response developed at the lower limbs is similar between the results obtained here and those reported by Nakashima et al. (2007), for the same swimming motion. However, a similar analysis is required for the remaining structures of the biomechanical model to ensure consistency with the expected behaviour of the human swimming motion. Nevertheless, the magnitude of the fluid forces computed for LHBM shows large discrepancies during some intervals of the stroke.

Regarding the results of the inverse dynamic analysis performed, these underly the importance of considering the whole system dynamics of the human lower limbs during front crawl swimming, and not only the feet. Despite the apparent consistency of some results, the analysis developed requires further validation, which is not possible at this stage due to lack of literature on the intersegmental forces of the lower limbs in the context of human swimming. Although the dynamic pattern estimated seems to represent the mechanisms of front crawl swimming in the lower limbs, with the major discrepancies occurring with the ankle joints, the intersegmental forces and joint torques are expected to be greater in this work because of the high hydrodynamic forces obtained during some phases of the stroke cycle, when compared to Nakashima et al. (2007). From the analysis of those intervals in the animation of Swumsuit, they correspond to situations in which the feet are not properly positioned relative to the adjacent body. The reason for that may be due to the movement performed by the swimmer, or a more plausible source of error is related with the rotations given in the simulation input file. The bad positioning has an immediate impact on the contact surface area of the feet with water, and thus in the generated joint forces since the vector of external forces is an explicit input of an inverse dynamic analysis.

The motion given as rotations of body segments in the joint motion input file is influenced by the order in which these rotations are written, which is to be expected since in 3D the rotations do not have the additive property. Considering that a Cartesian coordinates formulation is considered in this study, it becomes troublesome the transformation from Euler parameters to the rotation sequences expected by Swumsuit, especially due to the complexity and variety of segmental movements from upper to lower limbs. This may be a potential source of error on the estimation of fluid forces due to discontinuities in the rotation angles for some intervals of the analysis, thus suggesting that a more robust transformation of rotations should be identified.

References

Cohen, R. C. Z., Cleary, P. W., Mason, B. R., & Pease, D. L. (2015). The Role of the Hand During Freestyle Swimming. *Journal of Biomechanical Engineering*, *137*(11). https://doi.org/10.1115/1.4031586

Derrick, T. R., van den Bogert, A. J., Cereatti, A., Dumas, R., Fantozzi, S., & Leardini, A. (2020). ISB recommendations on the reporting of intersegmental forces and moments during human motion analysis. *Journal of Biomechanics*, *99*. https://doi.org/10.1016/j.jbiomech.2019.109533

Dumas, R., Chèze, L., & Verriest, J. P. (2007a). Adjustments to McConville et al. and Young et al. body segment inertial parameters. *Journal of Biomechanics*, *40*(3), 543–553. https://doi.org/10.1016/j.jbiomech.2006.02.013

Dumas, R., Chèze, L., & Verriest, J. P. (2007b). Corrigendum to "Adjustments to McConville et al. and Young et al. body segment inertial parameters" [J. Biomech. 40 (2007) 543-553]. *Journal of Biomechanics*, *40*(7), 1651–1652. https://doi.org/10.1016/j.jbiomech.2006.07.016

Harrison, S. M., Cohen, R. C. Z., Cleary, P. W., Mason, B. R., & Pease, D. L. (2014). Torque and power about the joints of the arm during the freestyle stroke. *12th International Symposium on Biomechanics and Medicine in Swimming*, 349–355.

Keys, M. (2010). *Establishing computational fluid dynamics models for swimming technique assessment*. PhD Thesis, School of Civil and Resource Engineering/School of Sports Science, Exercise and Health, The University of Western Australia.

Lauer, J., Rouard, A. H., & Vilas-Boas, J. P. (2016). Upper limb joint forces and moments during underwater cyclical movements. *Journal of Biomechanics*, *49*(14), 3355–3361. https://doi.org/10.1016/j.jbiomech.2016.08.027

Nakashima, M., Satou, K., & Miura, Y. (2007). Development of Swimming Human Simulation Model Considering Rigid Body Dynamics and Unsteady Fluid Force for Whole Body. *Journal of Fluid Science and Technology*, *2*(1), 56–67. https://doi.org/10.1299/jfst.2.56

Nikravesh, P. E. (1988). *Computer-Aided Analysis of Mechanical Systems* (P. Hall (ed.); First Edit). Englewood Cliffs, New Jersey.

Oliveira, H. (2016). *Inverse Dynamic Analysis of the Human Locomotion Apparatus for Gait*. MSc Thesis in Mechanical Engineering, Instituto Superior Técnico, Universidade de Lisboa.

Pàmies-Vilà, R. (2012). *Application of Multibody Dynamics Techniques to the Analysis of Human Gait*. PhD Thesis in Biomedical Engineering, Universitat Politècnica de Catalunya.

Quental, C., Folgado, J., Ambrósio, J. A. C., & Monteiro, J. (2015). Critical analysis of musculoskeletal modelling complexity in multibody biomechanical models of the upper limb. *Computer Methods in Biomechanics and Biomedical Engineering*, *18*(7), 749–759. https://doi.org/10.1080/10255842.2013.845879

Rajagopal, A., Dembia, C. L., DeMers, M. S., Delp, D. D., Hicks, J. L., & Delp, S. L. (2016). Full-Body Musculoskeletal Model for Muscle-Driven Simulation of Human Gait. *IEEE Transactions on Biomedical Engineering*, *63*(10), 2068–2079. https://doi.org/10.1109/TBME.2016.2586891

Sanders, R. H., Andersen, J. T., & Takagi, H. (2017). The Segmental Movements in Front Crawl Swimming. In B. Müller & S. I. Wolf (Eds.), *Handbook of Human Motion*. Springer, Cham. https://doi.org/10.1007/978-3-319-30808-1_132-1

Scott, S. H., & Winter, D. A. (1990). Internal forces at chronic running injury sites. *Medicine and Science in Sports and Exercise*, *22*(3), 357–369.

Silva, M. P. T., & Ambrósio, J. A. C. (2002). Kinematic data consistency in the inverse dynamic analysis of biomechanical systems. *Multibody System Dynamics*, *8*, 219–239. https://doi.org/10.1023/A:1019545530737

Takagi, H., Nakashima, M., Sato, Y., Matsuuchi, K., & Sanders, R. H. (2015). Numerical and experimental investigations of human swimming motions. *Journal of Sports Sciences*, *34*(16), 1564–1580. https://doi.org/10.1080/02640414.2015.1123284

Takagi, H., & Sanders, R. (2002). Measurement of propulsion by the hand during competitive swimming. *The Engineering of Sport*, *4*, 631–637.

Wei, T., Mark, R., & Hutchison, S. (2014). The Fluid Dynamics of Competitive Swimming. *Annual Review of Fluid Mechanics*, *46*, 547–565. https://doi.org/10.1146/annurev-fluid-011212-140658

Winter, D. A. (2009). *Biomechanics and Motor Control of Human Movement* (Fourth Edi). John Wiley & Sons, Inc. Hoboken, New Jersey. https://doi.org/10.1002/9780470549148

Wu, G., Siegler, S., Allard, P., Kirtley, C., Leardini, A., Rosenbaum, D., Whittle, M., D'Lima, D. D., Cristofolini, L., Witte, H., Schmid, O., & Stokes, I. (2002). ISB recommendation on definitions of joint coordinate system of various joints for the reporting of human joint motion - Part I: ankle, hip, and spine. *Journal of Biomechanics*, *35*(4), 543–548. https://doi.org/10.1016/s0021-9290(01)00222-6

Wu, G., van der Helm, F. C. T., Veeger, H. E. J., Makhsous, M., Van Roy, P., Anglin, C., Nagels, J., Karduna, A. R., McQuade, K., Wang, X., Werner, F. W., & Buchholz, B. (2005). ISB recommendation on definitions of joint coordinate systems of various joints for the reporting of human joint motion - Part II: shoulder, elbow, wrist and hand. *Journal of Biomechanics*, *38*(5), 981–992. https://doi.org/10.1016/j.jbiomech.2004.05.042